XXII. GASEOUS ELECTRONICS*

Academic and Research Staff

Prof. G. Bekefi
Prof. W. P. Allis
Prof. S. C. Brown
Prof. J. C. Ingraham
Prof. B. L. Wright
Dr. W. M. Manheimer
J. J. McCarthy
W. J. Mulligan

Graduate Students

W. B. Davis
G. A. Garosi
T. T. Wilheit, Jr.

RESEARCH OBJECTIVES

An ionized gas can provide a unique environment for populating atomic and molecular states. For this reason the gaseous electronics group continues to study fundamental atomic and molecular processes including measurements of cross sections and transport properties involving metastable states, molecular ions and free radicals. The experimental techniques include the use of microwaves, infrared and optical spectroscopy and lasers.

Since the distribution of charged particle velocities plays a dominant role in determining transport characteristics, much attention has been paid in the past to methods of establishing experimentally and theoretically the distribution function in steady-state and decaying plasmas.

In addition to the above, experimental and theoretical studies are carried out on the propagation of ion acoustic and diffusion waves, and on the effects of neutral gas turbulence on the electrical conductivity of partially ionized gases.

G. Bekefi

A. MEASUREMENT OF ELECTRON-NEUTRAL COLLISION FREQUENCIES IN AN ARGON PLASMA

In two previous reports, Ingraham[1,2] has reported and discussed a measurement of cesium electron-atom collision frequencies. Because of disagreement with other published work,[3] it is suggested that these data may be anomalous. In order either to gain confidence in the cesium data or to understand the anomaly a similar experiment is being being performed in argon.

1. Experiment

The experimental arrangement is shown in Figs. XXII-1 and XXII-2. It is both a transient absorption bridge and a transient radiometer. Thus the microwave absorption and the temperature can both be measured at any point in the discharge afterglow. Temperatures and absorptions are measured as a function of magnetic field strengths. Peak

*This work was supported by the Joint Services Electronics Programs (U.S. Army, U.S. Navy, and U.S. Air Force) under Contract DA 28-043-AMC-02536(E).

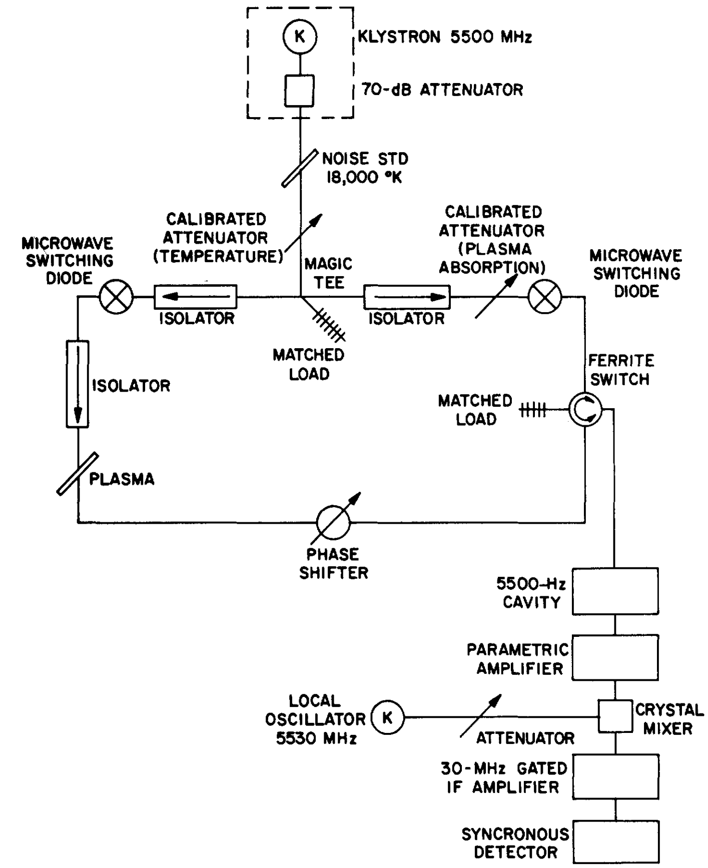

Fig. XXII-1. Experimental arrangement.

absorption occurs at electron-cyclotron resonance, and the value at the peak is typically from 0.1 dB to 10 dB for the 22-cm absorption length. Typical temperatures range from 300°K to 1500°K. If the measured temperature is independent of magnetic field, the electron velocity distribution is assumed to be Maxwellian.

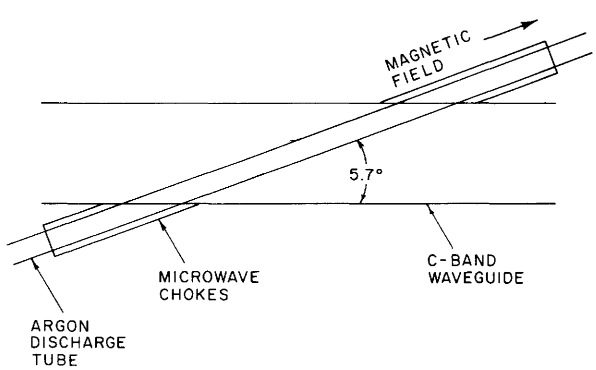

Fig. XXII-2. Detail of discharge tube and waveguide.

The operation of the apparatus has been described previously in detail by Ingraham.[1] Some changes have been made in the microwave circuit since it was previously described. The isolation of the adjacent channels of the ferrite switch is only approximately 20 dB. Because of the coherence of the two signals, this results in some sensitivity to the phase shift introduced by the plasma. To correct this, two microwave switching diodes have been added to give approximately 40 dB isolation. Reflections from the switching diodes made an additional isolator necessary. The phase sensitivity has been measured with the phase shifter in the plasma arm of the microwave bridge. We found it to be absent, within experimental error.

The cesium tube has been replaced with a sealed argon discharge tube. Pressures are changed by changing tubes.

The parametric amplifier was added to give added sensitivity in the temperature measurements. With this parametric amplifier the entire system has a noise figure around 4 dB.

2. Theoretical Considerations

In a previous report,[3] the author has sketched the derivation of the power absorption coefficient

$$\alpha = \frac{\omega_p^2\omega}{kc^2v_T ab}\int_0^{x^2+y^2=\rho^2} dxdy\,\sin^2\left(\frac{\pi y}{a}\right)\int \frac{d^3\vec{v}\,(v_x)^2\,\nu_c f_o}{\nu_c^2+(\omega-kv_z-\Omega)^2},$$

where ω_p is the electron plasma frequency $\left(n_o e^2/E_o m\right)^{1/2}$, and $v_T \doteq (KT/m)^{1/2}$. It was shown in the previous report[3] that the Doppler shift term, (kv_z), could be ignored for the experimental conditions in question. This left us with

$$\alpha = \frac{4\pi\omega_p^2\omega}{3kc^2v_T^2 ab}\int_0^{x^2+y^2=\rho^2} dxdy\,\sin^2\left(\frac{\pi y}{a}\right)\int_0^\infty \frac{dvv^4\,\nu_c f_o}{\nu_c^2+(\omega-\Omega)^2}.$$

The basic assumption made here is that the plasma does not significantly alter the waveguide fields. Clearly, this is true in the limit $\omega_p^2 \to 0$. But, in reality, ω_p^2 is not zero, so this expression for α is not exact. An exact calculation to second order in ω_p^2 would be extremely difficult. In this report, several heuristic models are presented in order to estimate possible second-order effects. These will be called, for lack of more descriptive names, "finite k_i effect," "upper hybrid effect," "phase velocity effect," and "dielectric rod effect."

a. Finite k_i Effect

Willett[4] has shown that if we allow for the fact that the attenuation length is finite, there is then an imaginary part to the propagation constant k, and a term similar to a Doppler shift arises

$$\alpha = \frac{\omega_p^2 \omega}{kc^2 v_T ab} \int_0^{x^2+y^2=\rho^2} dxdy \sin^2\left(\frac{\pi y}{a}\right) \int \frac{d^3\vec{v}\left(v_x^2\right) \nu_c f_o}{(\nu_c - k_i v_z)^2 + (\omega-\Omega)^2},$$

where k_i is the imaginary part of k. As in the previous report,[3] we can integrate over velocity directions and define a resonance function

$$\text{R. F.}(\omega-\Omega) = \frac{2}{k_i^2 v^2} - \left(\frac{(\omega-\Omega)^2 - \nu_c^2 + k_i^2 v^2}{2k_i^3 v^3 \nu_c}\right) \log\left\{\frac{(\omega-\Omega)^2 + (\nu_c - k_i v)^2}{(\omega-\Omega)^2 + (\nu_c + k_i v)^2}\right\}$$

$$- \frac{2(\omega-\Omega)}{k_i^3 v^3}\left\{\tan^{-1}\left(\frac{\nu_c + k_i v}{\omega-\Omega}\right) - \tan^{-1}\left(\frac{\nu_c - k_i v}{\omega-\Omega}\right)\right\}.$$

This has a half-width at half-maximum of approximately

$$\left[\nu_c^2 - 0.7(k_i)_o^2 v^2\right]^{1/2}$$

or in terms of a collision probability

$$\Delta_{1/2} \cong \left[P_c^2 p_o^2 - 0.7(k_i)_o^2\right]^{1/2} v,$$

where P_c is the collision probability at 1-Torr pressure, p_o is the pressure in Torr, and $(k_i)_o$ is the peak value of the imaginary part of the collision frequency. This gives a 1% error when $0.7(k_i)_o^2/P_o^2 p_o^2 = 0.02$. The minimum value for P_c for argon is approximately 0.5 cm^{-1} $Torr^{-1}$. In this experiment, $p_o = 10$ Torr. Thus, for 1% error, $k_i = 0.85$ cm^{-1}. In this experiment, the absorbing length is 22 cm, which corresponds to 160 dB power attenuation by the plasma. Therefore this effect is not large for 0.1-10 dB range of the present experiment.

b. Upper Hybrid Effect

In the calculation we have ignored the fact that the magnetic and propagation axes differ by 5.7° (see Fig. XXII-2). So, rather than have a resonance at the electron-cyclotron resonance frequency, we might expect the resonance to be that of a right-handed wave propagating at an angle of 5.7° to the magnetic field.

Allis, Buchsbaum, and Bers[5] give for the index of refraction of a right-handed wave in an electron plasma:

$$n^2 = 1 - \frac{2\left(\omega_p^2/\omega^2\right)\left(1-\omega_p^2/\omega^2\right)}{2\left(1 - \frac{\omega_p^2}{\omega^2}\right) - \frac{\Omega^2}{\omega^2}\sin^2\theta - D},$$

where

$$D^2 = \frac{\Omega^4}{\omega^4}\sin^4\theta + \frac{4\Omega^2}{\omega^2}\left(1 - \frac{\omega_p^2}{\omega^2}\right)^2\cos^2\theta.$$

For our case,

$$\frac{\Omega^4}{\omega^4}\sin^4\theta \ll \frac{4\Omega^2}{\omega^2}\left(1 - \frac{\omega_p^2}{\omega^2}\right)^2\cos^2\theta,$$

so

$$n^2 = 1 - \frac{\omega_p^2/\omega^2}{1 - \frac{(\Omega^2/\omega^2)\sin^2\theta}{2\left(1 - \frac{\omega_p^2}{\omega^2}\right)} - \frac{\Omega}{\omega}\cos\theta}$$

with $\Omega/\omega \approx 1$, and $\omega_p^2/\omega^2 \ll 1$; hence

$$n^2 = \frac{\omega_p^2/\omega^2}{1 - \Omega/\omega - \frac{1}{2}\left(\omega_p^2/\omega^2\right)\sin^2\theta}$$

with $\sin^2\theta = 0.0100$. Thus the resonant frequency for a right-handed wave propagating at 5.7° with respect to the magnetic field is $\Omega + 0.0005\ \omega_p^2/\omega$.

If we substitute this value in our expression for a, consider ω_p^2 a function of position, and approximate ν_c by a constant, we get

$$a = \frac{k_o^2}{k_g ab}\int \frac{dxdy\,\sin^2\left(\frac{\pi y}{a}\right)\omega_p^2(x,y)\ \nu_c}{\left(\omega - \Omega - 0.005\,\omega_p^2(x,y)/\omega^2\right)^2 + \nu_c^2}.$$

Approximate the plasma profile by

$$\omega_p^2(x,y) = \omega_{po}^2\left(1 - \frac{x^2+y^2}{p^2}\right) \quad \text{for } x^2+y^2 \leq p$$

$$\omega_p^2(x,y) = 0 \qquad\qquad \text{for } x^2+y^2 > p$$

Approximate $\sin^2(\pi y/a)$ by 1 for the region in which $\omega_p^2 \neq 0$.

$$\alpha = \frac{2k_o^2\omega_{po}^2\pi p^2}{abk_g\left(\omega_p^2/\omega\nu_c\right)}\left[\log\left\{1 + \frac{2.5\times 10^{-5}\left(\omega_p^2/\nu_c\omega\right)^2 - 10^{-2}\left(\frac{\Omega-\omega}{\nu_c}\right)\left(\frac{\omega_p^2}{\nu_c\omega}\right)}{\left(\frac{\omega-\Omega}{\nu_c}\right)^2+1}\right\}\right.$$
$$\left.+\,2\left(\frac{\Omega-\omega}{\nu_c}\right)\left\{\tan^{-1}\left(5\times 10^{-3}\left(\frac{\omega_p^2}{\omega\nu_c}\right) - \left(\frac{\Omega-\omega}{\nu_c}\right)\right) - \tan^{-1}\left(\frac{\Omega-\omega}{\nu_c}\right)\right\}\right].$$

Note that the absorption depends only on the dimensionless ratios $\left(\omega_{po}^2/\omega\nu_c\right)$ and $(\omega-\Omega/\nu_c)$. Thus for constant peak absorption the broadening is proportional to pressure (ν_c). This function was calculated numerically on an IBM 360/65 computer for the present experimental case (5.5 GHz in C-band waveguide), and for a 1-cm inner diameter of the discharge tube. The result may be scaled to other tube diameters by noting that the total peak absorption is proportional to the square of the inner diameter of the discharge tube. We found that the resonance is broadened by 1% for ~390 dB total absorption. In the data presented here, the discharge tube I. D. was 0.6 cm, so this is reduced to 1% broadening for ~110 dB absorption. Thus, once again, we have an effect that may be ignored in the present experiment.

c. Phase Velocity Effect

Notice that α is proportional to $\omega/k = v_p$, the phase velocity of the electromagnetic wave. The presence of the plasma does alter this phase velocity. If the waveguide were filled with a uniform isotropic dielectric, the dispersion relation would be $k^2 + \pi^2/a^2 = K\,\omega^2/c^2$

$$k = \sqrt{K\,\omega^2/c^2 - \pi^2/a^2},$$

where K is the dielectric coefficient. Consider the waveguide to be uniformly filled with plasma at an averaged density

$$\langle n\rangle = \frac{2}{ab}\int dxdy\; n(x,y)\,\sin^2\left(\frac{\pi y}{a}\right).$$

The weighting factor of $\sin^2(\pi y/a)$ occurs because the energy dissipation at any point is proportional to the square of the magnitude of the electric field strength. For the lowest waveguide mode (TE_{01}), the electric field has the form

$$\vec{E} = E_2\hat{x}\sin\left(\frac{\pi y}{a}\right)\cos(kz-\omega t).$$

For the dielectric constant K, take the diagonal part of the cold-plasma dielectric tensor.[5]

The resulting half-widths have been calculated numerically on an IBM 360/65 computer. Again the broadening is dependent only on the peak absorption. We found that 1% broadening occurred for a peak absorption of 15 dB. This may again be neglected in the present case.

d. Dielectric Rod Effect

In all of these models we have assumed that the interaction between the plasma and the electromagnetic wave was essentially that of a plane wave propagating through an infinite plasma. The actual geometry is quite the opposite, however. The dimensions

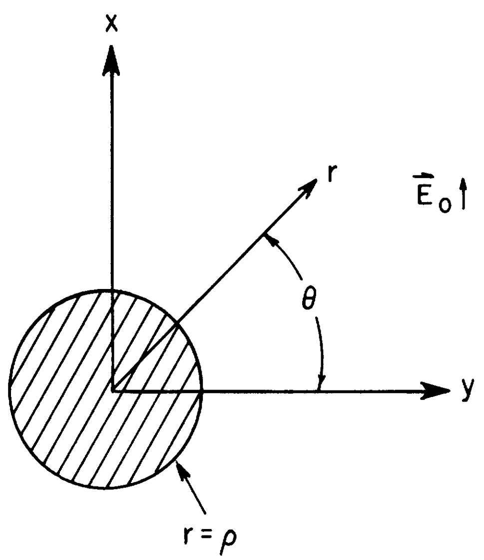

Fig. XXII-3. Two-dimensional dielectric rod problem.

of the plasma perpendicular to the direction of propagation are much smaller than a wavelength. The interaction can be modeled in the quasi-static approximation, in which we approximate the electric fields as the gradient of a scalar potential. We also approximate the plasma by a uniform rod of gyrotropic dielectric of radius P.

The resulting two-dimensional problem is illustrated in Fig. XXII-3. Let ϕ_1 be the scalar potential for $r > \rho$.

$$\phi_1 = -E_o r \sin\theta + \frac{A}{r}\sin\theta + \frac{B}{r}\cos\theta,$$

and for $r < \rho$,

$$\phi_2 = Cr \sin\theta + Dr \cos\theta.$$

For $r < \rho$, we have a two-dimensional dielectric tensor $\overleftrightarrow{K}$ such that

$$\vec{D} = \epsilon_o \overleftrightarrow{K}\, \vec{E}$$

$$\begin{pmatrix} D_x \\ D_x \end{pmatrix} = \epsilon_o \begin{pmatrix} K_\perp & -K_x \\ K_x & K_\perp \end{pmatrix} \begin{pmatrix} E_x \\ E_y \end{pmatrix}$$

Using continuity of ϕ and the normal component of $\vec{D}$ at the boundary $r = \rho$, we can determine the electric field inside the plasma.

$$\vec{E}_{\text{inside}} = \frac{2E_o[(1+K_\perp)\hat{x} - Kx\hat{y}]}{(1+K_\perp)^2 + (K_x)^2},$$

where $\hat{x}$ and $\hat{y}$ are unit vectors in the x and y directions, respectively. The rate of power absorption is proportional to $\vec{E}^* \cdot \overleftrightarrow{K} \cdot \vec{E}$. The values of $K_\perp$ and K_x, from Allis, Buchsbaum, and Bers,[5] are

$$K_\perp = 1 - \frac{\frac{1}{2}\frac{\omega_p^2}{\omega}}{\omega - \Omega + i\nu_c}$$

$$K_x = -\left(\frac{1}{2}\right) i \left\{\frac{\frac{\omega_p^2}{\omega}}{\omega - \Omega + i\nu_c}\right\}.$$

We find that the absorption is proportional to

$$\frac{\nu_c}{\left(\omega - \Omega + \frac{\omega_p^2}{2\omega}\right)^2 + \nu_c^2}.$$

Hence the resonance is shifted by an amount $\omega_p^2/2\omega$. To estimate the magnitude of this effect for the present measurements, we make the very crude approximation that this shifted resonance describes the absorption at each point in an inhomogeneous plasma. If we approximate the plasma profile by a parabola, we have an expression identical formally to the expression for the "upper hybrid effect." The

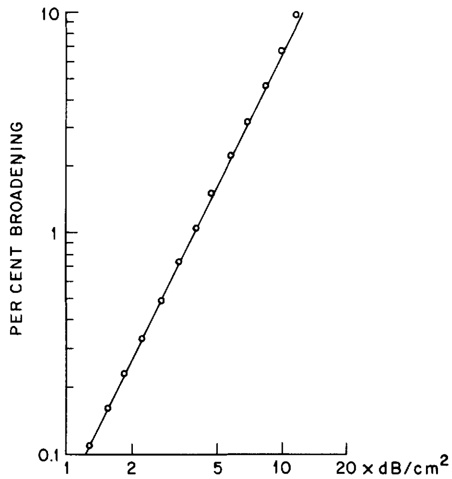

Fig. XXII-4. Broadening attributable to the "dielectric rod effect."

only difference is that we now get the same broadening for 1/100 of the density. That is, 1% broadening occurs for 3.9 dB for a 1-cm I.D. discharge tube. Similarly, for the 0.6 cm I.D. tube of the present experiments, 1% broadening occurs at 1.1 dB. This must be considered in evaluating the data. Figure XXII-4 is a plot of

$$x = \frac{\text{peak power absorption in dB}}{(\text{inner diameter of the discharge tube})^2}$$

against percentage of broadening.

3. Experimental Results

We shall consider the second-order effects negligible for peak absorption <2 dB. This gives ~4% error, because of the "dielectric rod effect." The other effects are smaller. We shall only use the data for which we can ignore these effects. A typical data run, showing absorption and temperature measurements versus magnetic field, is shown in Fig. XXII-5. In Fig. XXII-6, we show measured half-widths versus temperature for 20.0-Torr argon pressure. Ingraham[2] has calculated half-widths from the data of Frost and Phelps.[6] These are shown also in Fig. XXII-6. The dashed portion is an extrapolation; it was not calculated. Figure XXII-7 shows the same for 10.0-Torr pressure. The uncertainties in the half-widths are essentially the uncertainties in individual points near the half-maximum in the raw data.

Another way to analyze the data is to note that the ratio of the peak absorption

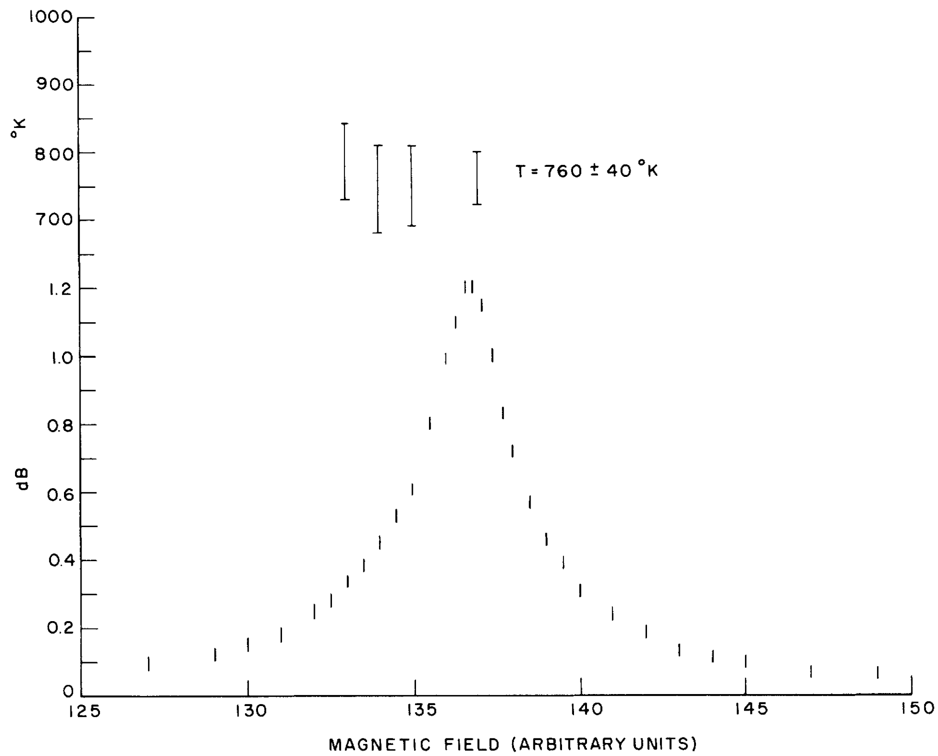

Fig. XXII-5. Typical data run.

to the area under the absorption curve is equal to

$$\frac{\pi \int \left(\nu_c^{-1}\right) v^4 f_o \, dv}{\int v^4 f_o \, dv} = \pi \left\langle \nu_c^{-1} \right\rangle .$$

Ingraham[2] has calculated these averages also. The data for 10.0 Torr and 20.0 Torr, respectively are shown and compared with Ingraham's calculations in Figs. XXII-8 and XXII-9. The large error bars result from approximating the contribution to the area under the curve from the unmeasured portions in the wings. We have assumed an $(\omega-\Omega)^{-2}$ dependence. A numerical fit of the form $A/(\omega-\Omega)^2 + \delta^2$, where A and δ are fitted to the data in the wing, would improve this.

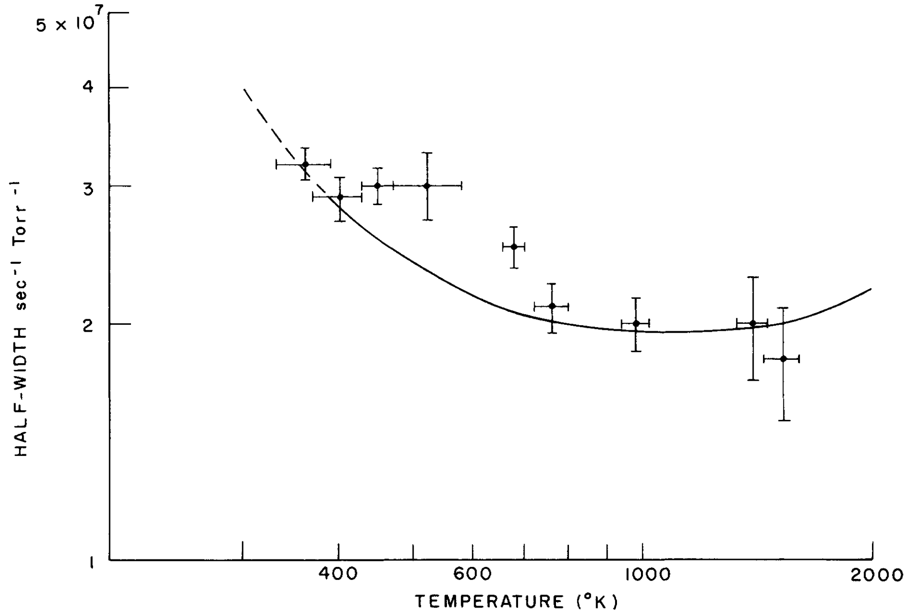

Fig. XXII-6. Half-width data for 20.0-Torr pressure.

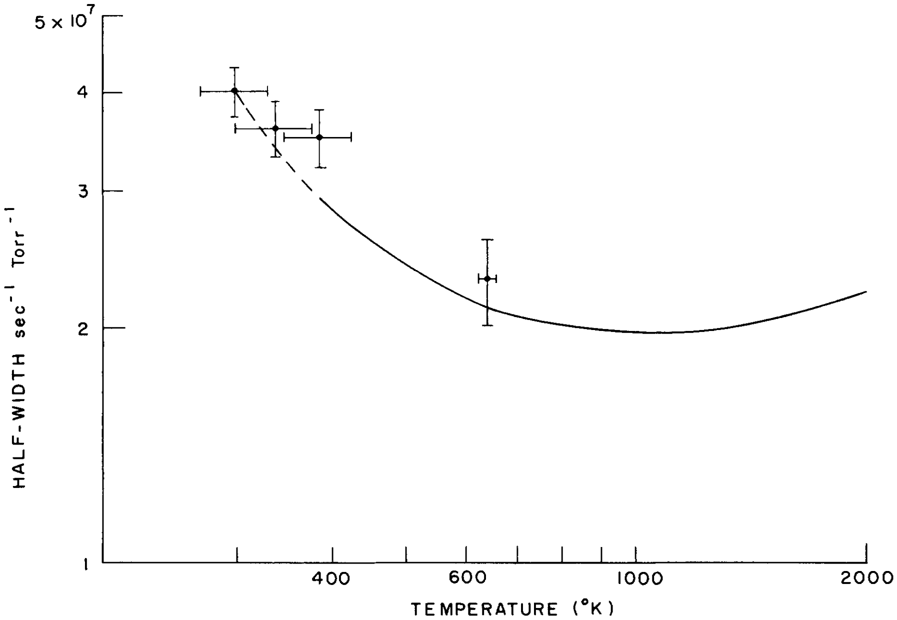

Fig. XXII-7. Half-width data for 10.0-Torr pressure.

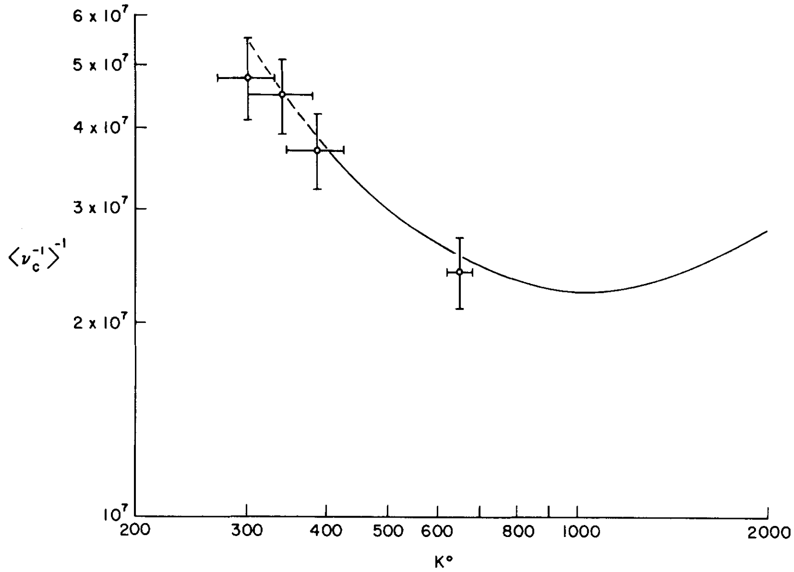

Fig. XXII-8. $\left\langle \nu_c^{-1} \right\rangle^{-1}$ data for 10.0-Torr pressure.

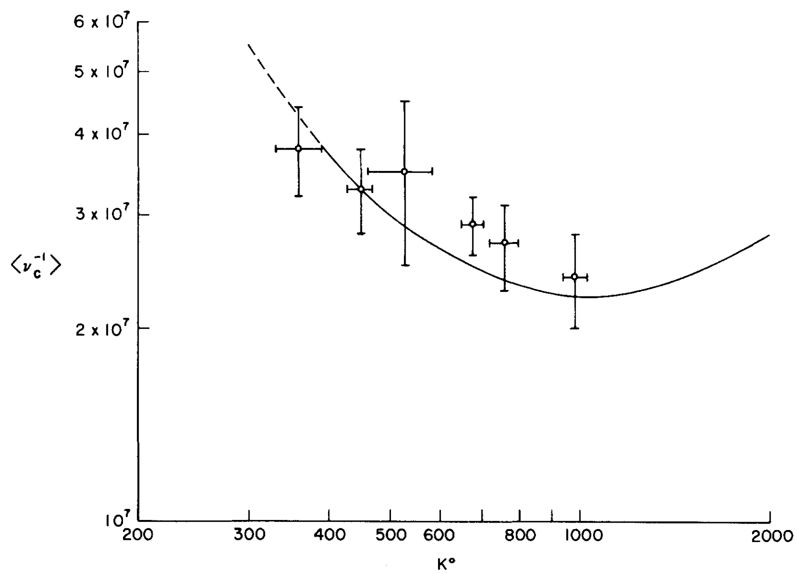

Fig. XXII-9. $\left\langle \nu_c^{-1} \right\rangle^{-1}$ data for 20.0-Torr pressure.

4. Conclusion

The agreement between calculations and measurements seems reasonably good. Certainly, if there were an anomaly in Ingraham's data, it is not present here. This gives added confidence to Ingraham's data, and, incidentally, to the argon data of Frost and Phelps.

T. T. Wilheit, Jr.

References

1. J. C. Ingraham, Quarterly Progress Report No. 77, Research Laboratory of Electronics, M.I.T., April 15, 1965, pp. 113-118.
2. J. C. Ingraham, Quarterly Progress Report No. 81, Research Laboratory of Electronics, M.I.T., April 15, 1966, pp. 63-67.
3. T. T. Wilheit, Jr., Quarterly Progress Report No. 86, Research Laboratory of Electronics, M.I.T., July 15, 1967, pp. 138-142.
4. J. E. Willett, J. Appl. Phys. 33, 898 (1962).
5. W. P. Allis, S. J. Buchsbaum and A. Bers, Waves in Anisotropic Plasmas (The M.I.T. Press, Cambridge, Mass., 1963).
6. L. S. Frost and A. V. Phelps, Phys. Rev. 136, A1538 (1964).